Tomographic Stress Profiling of Arc-Induced Long-Period Fiber Gratings

F. Dürr, G. Rego, P. V. S. Marques, Sergey L. Semjonov, Evgeny M. Dianov, *Member, IEEE*, H. G. Limberger, and R. P. Salathé, *Senior Member, IEEE*

***Abstract*—Long-period fiber gratings (LPGs) have been inscribed in nitrogen-doped fibers by electrical arc discharge. The influence of drawing tension as well as external load applied during arc discharge on coupling strength has been investigated. The influence of drawing tension on the grating's coupling strength is found to be negligible, whereas the coupling strength increases considerably with external load. Tomographic stress profiles of the fiber have been recorded before and after electric arc discharge. The axial stress modulation in the core region of the grating was found to be smaller than 10 MPa and is thus too small to be the dominating mechanism for grating formation.**

***Index Terms*—Arc discharges, gratings, optical fiber filters, stress measurement.**

I. Introduction

LONG-PERIOD fiber gratings (LPGs) are important components in modern all-fiber devices and systems used for optical communication networks. For instance, LPGs find application as gain equalizers in broadband erbium-doped fiber amplifiers [1], as filters in Raman amplifiers and lasers [2], and as band rejection filters [3]. Periodic modulation of the fiber's index profile allows coupling from the core mode to discrete lossy cladding modes of the fiber, resulting in several rejection peaks in the transmission spectrum with negligible back reflection [4]. The position of the rejection peaks is determined by the grating period as well as the effective indices of the core and the cladding modes, whereas the peak strength is proportional to the overlap of the two involved mode fields with the index perturbation.

Different techniques have been reported within the last decade to achieve the necessary changes in the index profile. Most commonly, fiber cores are exposed to ultraviolet laser irradiation, either using an amplitude mask [3] or a point-by-point technique [5], resulting in a local increase of the doped core glass refractive index. This method is highly flexible, as it allows arbitrary adjustment of the period and a wide range of core refractive index changes. However, the UV-induced index change may decrease considerably during the lifetime of the grating [3]. To avoid device degradation, annealing methods [6] must be applied after the UV exposure, complicating the fabrication process and increasing device cost.

Ultrashort laser sources have been used alternatively for the fabrication of LPGs. In 1999, Kondo *et al.* reported the first realization of LPGs by focusing 810-nm femtosecond-laser pulses on the fiber core [7]. Recently, high-quality gratings with excess loss of less than 0.15 dB have been fabricated using this technique [8]. However, due to the nonlinear interaction process between the laser pulses and the fiber core glass, the correct alignment of the fiber with respect to the pulse train is a crucial and difficult issue, complicating the fabrication process considerably.

The origins of index changes induced by UV as well as femtosecond-laser irradiation have not been clarified in detail so far. It is widely accepted that the index change comprises two different parts, one part caused by a modification of defects in the fiber glass ("color-center model") [9], another part induced by a densification of the irradiated doped core glass [10]. The densification results in an increase in core stress for UV-irradiated [10], [11] as well as for 810-nm femtosecond-laser-induced [12] gratings.

Complementary LPG fabrication techniques based on thermal effects have been developed. The writing of LPGs using CO_2 lasers emitting in the mid-infrared has been reported recently [13]. Kim *et al.* measured the residual stress in the fiber as a function of axial position and concluded that the refractive index change in such kind of gratings can be attributed to a release of fiber core stress due to heating with the focused laser beam [14], [15]. Refractive index and stress are related by photoelasticity; an increase in core stress results in a decrease in core refractive index and vice versa [11], [15].

An alternative and cost-efficient method for LPG fabrication is the periodic exposure of the fiber to an electric arc discharge [16]. Using this technique, LPGs have been realized in a multitude of single-mode optical fibers, differing basically in core dopant [17]. Recently, arc-induced LPGs have also been fabricated in a photonic crystal fiber [18]. However, as for UV- and femtosecond-laser-irradiated fibers, the origins of the arc-induced perturbations have not been identified in detail so far. Several mechanisms, including dopant diffusion

Manuscript received April 11, 2005; revised June 28, 2005. This work was supported by the ODUPE Research Training Network of the European Commission, under Contract HPRN-CT-2000-00045. The work of G. Rego was supported by the grant conceded by the Program PRODEP III.

F. Dürr, H. G. Limberger, and R. P. Salathé are with the Ecole Polytechnique Fédérale de Lausanne, Advanced Photonics Laboratory, CH-1015 Lausanne, Switzerland (e-mail: hans.limberger@epfl.ch).

G. Rego is with the Escola Superior de Tecnologia e Gestão, 4900-348 Viana do Castelo, Portugal, and also with the Unidade de Tecnologia Optoelectrónica e Electrónica, INESC Porto, 4169-007 Porto, Portugal.

P. V. S. Marques is with the Unidade de Tecnologia Optoelectrónica e Electrónica, INESC Porto, 4169-007 Porto, Portugal, and also with the Departamento de Física, 4169-007 Porto, Portugal (e-mail: psmarque@fc.up.pt).

S. L. Semjonov and E. M. Dianov are with the Fiber Optics Research Center, General Physics Institute, Russian Academy of Science, 119991 Moscow, Russia.

Digital Object Identifier 10.1109/JLT.2005.857763

[16], [19], [20], stress relaxation [21], [22], geometrical deformation [16], [23], [24], as well as changes in glass structure [17], [18], have been suggested, mostly without providing any experimental evidence. Depending on writing conditions, only one or more mechanisms perturbing the index profile might occur. It is thus of high interest to identify each mechanism and to clarify its impact on grating formation. In this context, the goal of this work is to get insight in the influence of stress changes on the overall mechanism.

II. Experiment

A. Fibers Under Investigation

Three nitrogen-doped fibers have been investigated within this study. The fibers were drawn from the same preform at different drawing tensions. The preform has been manufactured by reduced-pressure plasma-chemical deposition [25]. The nitrogen-doped core layers incorporate 1 at% of nitrogen and are deposited in a pure silica supporting tube, which itself is embedded into several pure silica jacketing tubes. Drawing tensions of 65, 125, and 195 g, respectively, were used, corresponding to drawing temperatures of 1940, 1905, and 1880 °C at constant drawing speed. The difference in drawing tension results in different residual stress profiles due to a mismatch in core and cladding viscosity at the drawing temperature [26]. The core and cladding diameters of the three fibers were measured using a Photon Kinetics 2400 Fiber Geometry System and found to be 6.0 ± 0.2 μm and 126.0 ± 0.3 μm, respectively. Refractive index near field measurements yield a core–cladding index difference of $(1.10 \pm 0.06) \times 10^{-2}$ for all fibers under investigation. The photoelastic contribution to the refractive-index difference [27] was hence too small to be detected within the error of the refractive-index measurement.

B. LPG Inscription

For LPG inscription, the respective fiber was mounted between the electrodes of a conventional splicing machine (BICC AFS3100). Therefore, one end of the fiber was clamped in a V-groove fiber holder on top of a motorized translation stage and a weight was attached to the other end of the fiber to keep it under tension. To evaluate the influence of this external load on the grating spectrum, three different weights (5.1, 22.8, and 36.3 g) have been used within the experiment. An electric arc was applied to the fiber using a current of 9 mA and a discharge time of 1 s for all gratings. The resulting peak temperature and full-width at half-maximum (FWHM) of the temperature distribution in the fiber during the discharge was estimated to be about 1320 °C and 1.6 mm, respectively [28]. After each arc discharge, the fiber was moved by one grating period before the next discharge was applied. Thus, a periodic perturbation of the fiber was achieved, which resulted in the desired coupling behavior of the grating. For all gratings, a period of 400 μm was chosen and 40 discharges were applied to the fiber, resulting in a total grating length of 16 mm. The LPG transmission spectra have been recorded using a white-light source and an optical spectrum analyzer with a wavelength resolution of 1 nm.

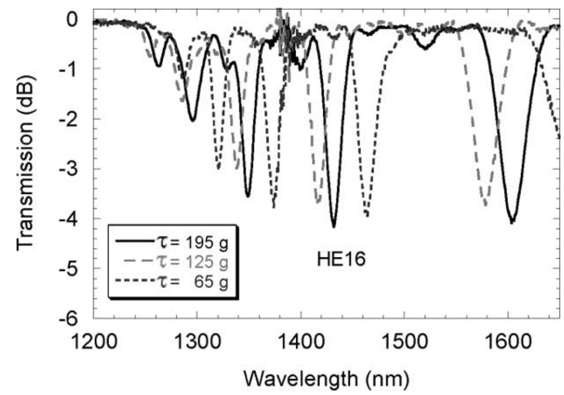

Fig. 1. LPG spectra obtained for grating inscription in fibers drawn at different drawing tensions using arc discharge. The external load was set to 22.8 g.

C. Tomographic Stress Measurements

To determine the two-dimensional stress profile of the fibers, a setup similar to the one presented in [29] has been installed. The axial-stress-induced phase-retardation profile of the fiber is determined polarimetrically for 60 projection angles from 0° to 180°. Subsequently, the axial stress profile is calculated from the projection data by an inverse Radon transform [30]. The imaging system used consists of a 10× objective $(\mathrm{NA} = 0.3)$ and a charge-coupled device (CCD) camera (768 × 574 pixels). The sampled area in the object plane has a size of about 520×390 μm^2. In the vertical direction, the area is divided into seven rows of 82 pixels. To improve the signal-to-noise ratio, we average over the 82 pixels, resulting in seven sampling points with a resolution of about 55 μm along the fiber axis. The transverse spatial resolution is given by the diffraction limit of the objective and is about 1.3 μm.

III. Results

A. LPG Inscription

To investigate the influence of fiber drawing tension on the grating spectra, LPGs have been written in each of the three fibers using exactly the same arc-discharge parameters. The external load applied to the fiber was set to 22.8 g. The three grating spectra obtained are shown in Fig. 1. For each of the three fibers, five loss peaks in the transmission spectrum can be identified. The corresponding change in core refractive index was found by comparing the spectra with simulated data obtained by calculations using the IFO_Gratings software package from Optiwave. For sinusoidal modulation, the core index was found to have an amplitude of about 3×10^{-4}. No significant dependence of peak loss or coupling strength on drawing tension could be observed within the reproducibility of the grating-fabrication method. In contrast, the peak positions were found to differ significantly for the three fibers under investigation. However, no correlation was found between peak position and drawing tension.

In addition, LPGs have been inscribed using three different external loads. All gratings were written in the fiber drawn with the lowest drawing tension of 65 g. The corresponding grating spectra are shown in Fig. 2. The loss peaks have been assigned

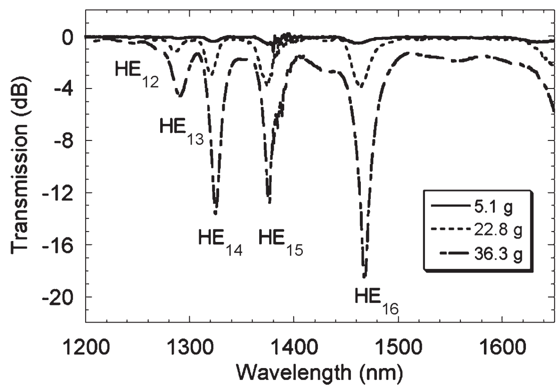

Fig. 2. LPG spectra obtained for grating inscription with varying external load in the fiber drawn with the lowest drawing tension of 65 g.

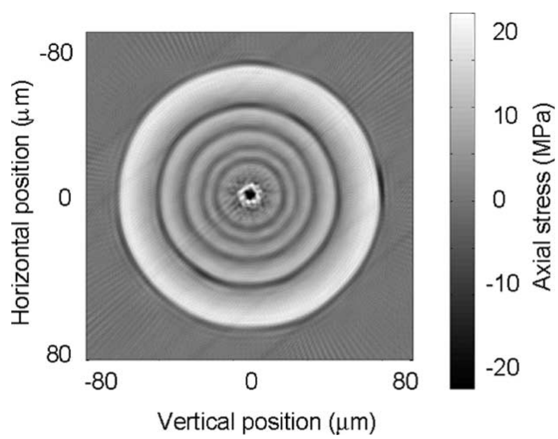

Fig. 3. Tomographic stress profile of the nitrogen-doped fiber drawn with a tension of 125 g.

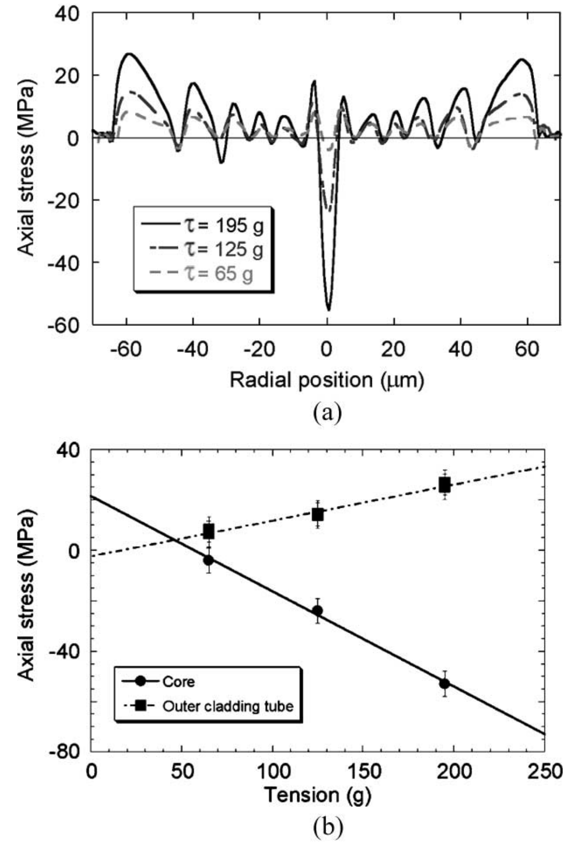

Fig. 4. (a) Residual stress profiles of the three fibers drawn at different tensions. (b) Core and cladding tube stress change with drawing tension.

to the corresponding cladding modes. The peak positions of the gratings do not depend on external load, whereas the peak transmission losses increase with increasing external load. Rejection losses of the HE_{16} resonance vary from -18.5 to -0.55 dB with external loads of 5.1 to 36.6 g. For the highest external load, an excess loss of about -2 dB is found; in contrast, the excess loss in the two other LPGs does not exceed -0.25 dB.

B. Tomographic Stress Measurement

To get direct information about stress changes due to arc discharge, tomographic stress measurements have been performed in the fibers before and after grating inscription. A typical stress profile obtained is illustrated in Fig. 3 for the fiber drawn with a tension of 125 g. Before discharge, the stress profiles of all fibers are found to be symmetric.

One-dimensional stress profiles of the three pristine fibers are illustrated in Fig. 4(a). The fiber cores are under compressive stress, whereas the surrounding silica tubes exhibit tensile stress. Fig. 4(b) shows the core and outermost cladding tube stresses plotted as a function of drawing tension. As expected, a linear dependence of stress on drawing tension is found [26]. Extrapolation to zero drawing tension yields the stress values of the preform, where only thermal stresses are present. If drawing-induced stresses were annealed completely after arc discharge, the fiber stress profile would equal the preform stress profile with a tensile core stress of about 20 MPa and an almost vanishing stress value in the cladding. For the fiber drawn with the highest tension of 195 g, where the initially compressive core stress is almost -60 MPa, a stress modulation of up to 80 MPa could thus be achieved theoretically, corresponding to a potential index modulation of 5.2×10^{-4} [11], which is indeed sufficient for grating realization.

After the arc discharge, the stress profile has been changed considerably. In Fig. 5, two-dimensional (2-D) stress profiles of the fibers drawn with a tension of 195 g (above) and 65 g (below) are shown after LPG inscription. For both cases, the externally applied load during arc discharge was set to 22.8 g. The stress in the fiber exhibits mirror symmetry along the axis of arc discharge. The stress profiles do not depend on the initial stress profile, neither at the position of arc discharge ("mark"), nor in-between two adjacent arc-discharge positions ("space"). The initially compressive core stress has been annealed to a tensile stress of 15 MPa in the "mark" and 10 MPa in the "space" region, respectively. For both "mark" and "space," the fiber stress at the air–cladding interface has turned compressive.

In Fig. 6, the modification of axial stress with external load applied to the fiber during discharge is shown for the fiber drawn with the highest tension. Again, we find stress modifications with mirror symmetry along the axis of arc discharge both in the "mark" (left column) and in the "space" (right column) regions of the LPG. Clearly, the quantity of residual stress in the cladding increases with external load for both regions. The residual stress in the "space" region is almost twice as large as

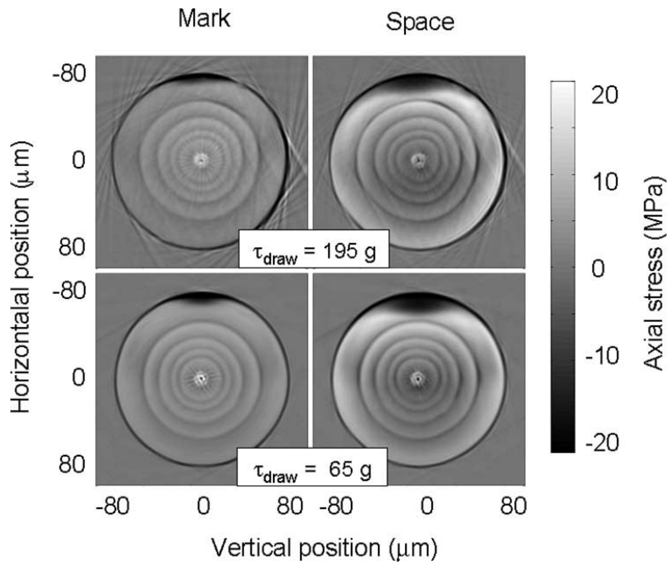

Fig. 5. Arc-induced two-dimensional stress profiles of the nitrogen-doped fiber for drawing tensions of 195 g (above) and 65 g (below). External load applied to both fibers was 22.8 g. The left and right columns show the profile at the position of arc discharge and in the middle of two discharges, respectively. Almost no dependence on the initial stress profile is found.

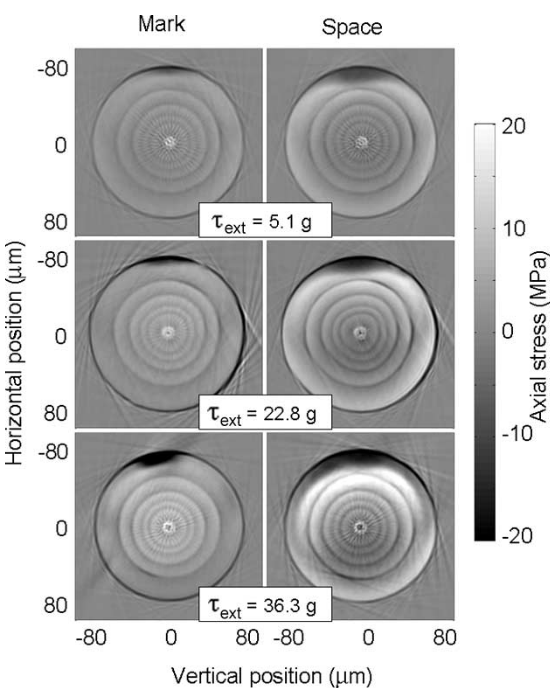

Fig. 6. Arc-induced two-dimensional stress profiles of nitrogen-doped fiber ($\tau_{\mathrm{draw}} = 195$ g) as a function of external load applied during discharge (5.1 g above, 22.6 g middle, 36.6 g below). The higher the external load, the higher is the residual stress in the cladding.

in the "mark" region. However, the residual core stress is only slightly affected by the external load. For all loads, the residual core stress is approximately 15 MPa in the "mark" and about 10 MPa in the "space" region.

IV. Discussion

The results reported in the previous section allow us to get substantial information about the contribution of stress changes to the LPG-formation process. As the three fibers under investigation were drawn from the same preform, they should have almost the same dopant concentration profile. In contrast, as shown in Fig. 4(a), the fibers exhibit significantly different stress profiles. The larger the drawing tension, the stronger is the compressive core stress. If stress relaxation was the mechanism dominating the grating-formation process, the strength of the LPG rejection peaks should increase with fiber drawing tension. For higher drawing tension, more stress can potentially be annealed by the discharge [Fig. 4(b)], resulting in a higher photoelastic index change. However, as illustrated in Fig. 1, there is no significant dependence of rejection peak strength on drawing tension. Only the position of the peaks changes significantly for the three fibers. We attribute the difference in peak position to the small differences in core and cladding diameter. The tomographic measurements presented in Fig. 5 confirm the negligible impact of initial stress on the grating-formation mechanism. The two fibers with different initial stress exhibit nearly identical stress profiles after arc discharge. In both the "mark" and the "space" regions, the core stress has been almost completely annealed. The remaining modulation of core stress between the two regions is smaller than 10 MPa, corresponding to a core index modulation amplitude of less than -3.25×10^{-5} [11], and is thus almost one order of magnitude too small to cause the rejection peak strength illustrated in Fig. 1.

The magnitude of external load is crucial for the LPG coupling strength, as depicted in Fig. 2. The higher the external load, the higher is the rejection peak strength. The corresponding 2-D stress profiles are illustrated in Fig. 6. Again, as for the gratings presented in Fig. 5, the stress modulation of the core remains smaller than 10 MPa. Thus, the corresponding change in refractive index is again too small to cause the index perturbation responsible for grating formation. The amplification of coupling strength with external load (Fig. 2) cannot be explained by core stress changes.

In the cladding tubes, an increase of remaining stress with external load is observable (Fig. 6). The corresponding changes in refractive index alter the effective indices of cladding modes, which, in general, are sensitive to even small perturbations of the index profile. Due to the asymmetry of the profiles, the external load might therefore affect the polarization properties of the grating [31]. Possible explanations for the asymmetry are an inhomogeneous temperature distribution in the arc and/or the occurrence of shear stress in the fiber due to a misalignment, as reported for the grating-formation process in [32].

It is clear from Figs. 5 and 6 that the external load applied to the fiber, rather than the initial stress profile, determines the amount of residual cladding stress after arc discharge. This implies that the initial stress profile is replaced by another stress profile, which is basically determined by the external load applied to the fiber: The higher the external load, the higher the residual stress. There are, in principle, two possibilities for the external load to influence the residual stress. It might hamper the stress annealing for temperatures above the annealing point, or introduce new stress, comparable to drawing-induced stresses, when the temperature reaches the softening point. Glass viscosities of $10^{13.4}$ and $10^{7.6}$ define the annealing

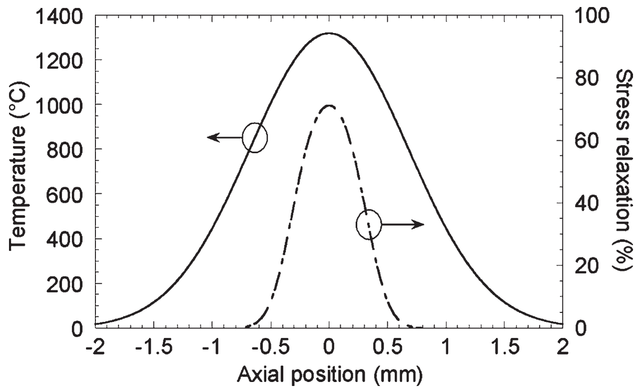

Fig. 7. Temperature distribution [28] and corresponding stress relaxation [35] for a single arc discharge.

and softening point of glass [33]. For silica, the corresponding temperatures are about 1150 and 1650 °C, respectively [34]. The approximate temperature of 1320 °C induced by the arc in the fiber is considerably below the softening point. We thus suggest at this point that the higher residual stress for increasing external load is caused by a stress-induced slowdown of annealing. The external load inhibits further stress relaxation by keeping the fiber under constant elongation. However, to corroborate this assumption, a more detailed analysis of the influence of externally applied stress on annealing is necessary.

From the temperature profile of the arc [28], the dependence of stress relaxation on axial position can essentially be determined by extrapolating the data presented by Mohanna *et al.* in [35] for temperatures below 1080 °C. The stress relaxation in optical fibers is governed by

$$\frac{\sigma}{\sigma_0} = \exp\left[-(at)^b\right] \tag{1}$$

where σ_0 is the initial stress, t the annealing time, $a = \exp[19.78 - 2.45 \times 10^4 \times (1/T)]\,\mathrm{min}^{-1}$ with T in kelvin, and b is 0.68 for high temperatures. Both temperature and stress relaxation are illustrated as a function of axial position in Fig. 7. The $1/\mathrm{e}^2$ full width of the stress-annealed region is about 1 mm. The discharge time used to calculate the stress relaxation is 1 s. For a given period of the LPG, the axial temperature modulation due to arc discharge as well as the corresponding stress relaxation can be determined from Fig. 7. The maximum temperature of 1320 °C occurs at the position of discharge, whereas the smallest temperature of about 1270 °C is reached midway between two discharges, i.e., at a distance of 200 μm from the maximum for a period of 400 μm. The peak-to-peak temperature modulation thus only yields about 50 °C with corresponding stress relaxations of 71% and 57%, respectively.

To confirm these theoretical predictions based essentially on the assumed discharge temperature by experiment, the stress-measurement setup was used as a polarization microscope to get the birefringence information as a function of axial position for a fiber subjected to a single arc discharge (Fig. 8). The higher the contrast between fiber and surrounding index liquid in Fig. 8, the higher is the remaining stress in the fiber. The

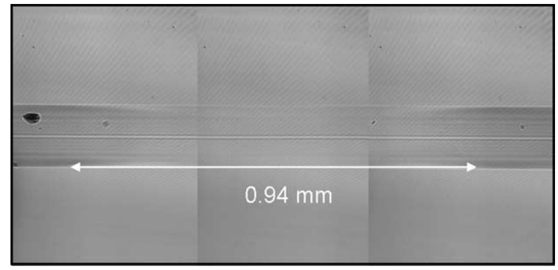

Fig. 8. Stress relief after a single arc discharge. The length of the annealed region is about 0.94 mm.

length of the stress-annealed region can thus be estimated to be about 0.94 mm, which is in good agreement with the theoretical value illustrated in Fig. 7.

Our results basically agree with results about stress transformation due to fusion splicing reported in [36]. There, complete annealing of drawing-induced stress was reported for a region of about 1.5 mm in length after arc discharge. The region of complete stress annealing is about 50% smaller in our case, as illustrated in Fig. 8. We attribute this difference to different discharge conditions used in our experiment.

Since the distance between two adjacent discharge positions within the grating is only 400 μm, there is a strong overlap between the stress-annealed regions, resulting in an almost negligible modulation of core stress, as found in Figs. 5 and 6. For LPGs with larger period, we expect a stronger contribution of stress modification to the grating-formation process. Indeed, we could observe loss peaks with double strength for gratings written with a period of 540 μm and a fourfold increase in coupling strength for a period of 680 μm. We thus conclude that, if the grating period is large enough, stress annealing can also enhance the coupling strength in arc-induced LPGs.

So far, we still lack an explanation for the LPG-formation mechanism and its sensitivity to the external load. Periodic diameter reductions, as reported in [24], could be observed in the LPGs written with the two higher external loads using an optical microscope. For the LPG written with an external load of 22.8 g, the fiber diameter decreased by $\sim$ 5% at the position of discharge, the LPG written with 36.3 g showed reductions of about 10%. The diameter changes of the fiber will, in principle, also affect the core geometry. The resulting change in the refractive-index profile could thus be the origin of the coupling of the fundamental core mode to cladding modes. The strong amplification of coupling strength with external load (Fig. 2) strongly supports this assumption. However, a systematic modeling of the influence of core-diameter changes on coupling strength is necessary to corroborate this hypothesis.

From the amount of diameter reduction for a given external load, we can reevaluate the maximum temperature in the region of discharge. The change of diameter with external load is given by [37]

$$\frac{1}{r}\frac{\mathrm{d}r}{\mathrm{d}t} = -\frac{p}{\eta} \tag{2}$$

where r is the fiber radius, p the pulling stress in newtons per square meter, η the viscosity, and t the time. For diameter reductions of 10% and 5% at corresponding external loads of 36.3 and 22.8 g, we find viscosities of $\lg(\eta) = 9.46$ and 9.56, respectively. Following Doremus [34], the temperature value associated with these viscosities is around 1400 °C, which is in reasonable agreement with the assumed peak temperature of 1320 °C.

As another possible mechanism for grating formation, dopant diffusion in the region of discharge has been suggested [20]. For nitrogen-doped fibers, the fabrication of mode field converters and LPGs by thermodiffusion has been reported in [19]. However, the heating times used within this study are much shorter. For a temperature of 1500 °C, no dopant diffusion could be observed in nitrogen-doped fibers after annealing for 3 h [38]. In addition, if diffusion would occur for the short times reported here, we would expect a significant correlation of core diameter with drawing temperature, which could not be observed. We thus estimate the influence of dopant diffusion to the grating-formation process to be negligible.

V. Conclusion

Long-period fiber gratings (LPGs) have been inscribed in nitrogen-doped fibers by electrical arc discharge. The influence of drawing tension as well as external load applied during arc discharge on the grating coupling strength has been investigated. For the grating period used within this study, the influence of drawing tension on coupling strength is found to be negligible, whereas coupling strength increases considerably with external load applied during discharge. Tomographic stress profiles of the fiber have been recorded before and after electric arc discharge. The axial stress modulation of the affected core region was found to be smaller than 10 MPa and is thus too small to be the dominating mechanism for grating formation.

We conclude that for LPGs, where the full-width at half-maximum (FWHM) of the heating source is larger than the grating period, the effect of stress annealing on grating formation is negligible. Grating formation is mainly governed by a periodic diameter reduction of the fiber, which can be reinforced by an external load. However, when the FWHM of the heating source is smaller than the grating period, residual stress relaxation may dominate the coupling strength. For high external loads applied to the fiber, we nevertheless expect the diameter reduction to have a significant impact on the grating-formation process. The grating-formation process is thus basically independent of the fiber dopant. In any case, to identify clearly the different mechanisms as a function of different writing parameters, a detailed comparison of experimental data with simulated data is crucial.

Acknowledgment

The authors would like to gratefully acknowledge helpful discussions with C. R. Kurkjian, F. Cochet, and S. A. Vasiliev about dopant diffusion in optical fibers.

References

[1] A. M. Vengsarkar, J. R. Pedrazzani, J. B. Judkins, P. J. Lemaire, N. S. Bergano, and C. R. Davidson, "Long-period fiber-grating-based gain equalizers," *Opt. Lett.*, vol. 21, no. 5, pp. 336–338, 1996.

[2] Y. G. Han, C. S. Kim, J. U. Kang, U. C. Paek, and Y. Chung, "Multiwavelength Raman fiber-ring laser based on tunable cascaded long-period fiber gratings," *IEEE Photon. Technol. Lett.*, vol. 15, no. 3, pp. 383–385, Mar. 2003.

[3] A. M. Vengsarkar, P. J. Lemaire, J. B. Judkins, V. Bhatia, T. Erdogan, and J. E. Sipe, "Long-period fiber gratings as band-rejection filters," *J. Lightw. Technol.*, vol. 14, no. 1, pp. 58–65, Jan. 1996.

[4] T. Erdogan, "Cladding-mode resonances in short- and long-period fiber grating filters," *J. Opt. Soc. Amer. A*, vol. 14, no. 8, pp. 1760–1773, 1997.

[5] K. O. Hill, B. Malo, K. A. Vineberg, F. Bilodeau, D. C. Johnson, and I. Skinner, "Efficient mode conversion in telecommunication fiber using externally written gratings," *Electron. Lett.*, vol. 26, no. 16, pp. 1270–1272, Aug. 1990.

[6] T. Erdogan, V. Mizrahi, P. J. Lemaire, and D. Monroe, "Decay of ultraviolet-induced fiber Bragg gratings," *J. Appl. Phys.*, vol. 76, no. 1, pp. 73–80, 1994.

[7] Y. Kondo, K. Nouchi, T. Mitsuyu, M. Watanabe, P. G. Kazansky, and K. Hirao, "Fabrication of long-period fiber gratings by focused irradiation of infrared femtosecond laser pulses," *Opt. Lett.*, vol. 24, no. 10, pp. 646–648, 1999.

[8] F. Hindle, E. Fertein, C. Przygodzki, F. Dürr, L. Paccou, R. Bocquet, P. Niay, H. G. Limberger, and M. Douay, "Inscription of long-period gratings in pure silica and germano-silicate fiber cores by femtosecond laser irradiation," *IEEE Photon. Technol. Lett.*, vol. 16, no. 8, pp. 1861–1863, Aug. 2004.

[9] J. Nishii, "Permanent index changes in Ge-SiO_2 glasses by excimer laser irradiation," *Mat. Sci. Eng., B*, vol. B54, no. 1–2, pp. 1–10, 1998.

[10] P. Y. Fonjallaz, H. G. Limberger, R. P. Salathe, F. Cochet, and B. Leuenberger, "Tension increase correlated to refractive-index change in fibers containing UV-written Bragg gratings," *Opt. Lett.*, vol. 20, no. 11, pp. 1346–1348, 1995.

[11] H. G. Limberger, P. Y. Fonjallaz, R. P. Salathe, and F. Cochet, "Compaction- and photoelastic-induced index changes in fiber Bragg gratings," *Appl. Phys. Lett.*, vol. 68, no. 22, pp. 3069–3071, 1996.

[12] F. Dürr, H. G. Limberger, R. P. Salathé, F. Hindle, M. Douay, E. Fertein, and C. Przygodzki, "Tomographic measurement of femtosecond-laser induced stress changes in optical fibers," *Appl. Phys. Lett.*, vol. 84, no. 24, pp. 4983–4985, 2004.

[13] D. D. Davis, T. K. Gaylord, E. N. Glytsis, S. G. Kosinski, S. C. Mettler, and A. M. Vengsarkar, "Long-period fibre grating fabrication with focused CO_2 laser pulses," *Electron. Lett.*, vol. 34, no. 4, pp. 302–303, Feb. 1998.

[14] B. H. Kim, Y. Park, T. J. Ahn, D. Y. Kim, B. H. Lee, Y. Chung, U. C. Paek, and W. T. Han, "Residual stress relaxation in the core of optical fiber by CO_2 laser irradiation," *Opt. Lett.*, vol. 26, no. 21, pp. 1657–1659, 2001.

[15] B. H. Kim, T. J. Ahn, D. Y. Kim, B. H. Lee, Y. Chung, U. C. Paek, and W. T. Han, "Effect of CO_2 laser irradiation on the refractive-index change in optical fibers," *Appl. Opt.*, vol. 41, no. 19, pp. 3809–3815, 2002.

[16] S. G. Kosinski and A. M. Vengsarkar, "Splicer-based long-period fiber gratings," in *Proc. Optical Fiber Communication (OFC)*, San Diego, CA, 1998, pp. 278–279.

[17] G. Rego, O. Okhotnikov, E. M. Dianov, and V. B. Sulimov, "High-temperature stability of long-period fiber gratings using an electric arc," *J. Lightw. Technol.*, vol. 19, no. 10, pp. 1574–1579, Oct. 2001.

[18] K. Morishita and Y. Miyake, "Fabrication and resonance wavelengths of long-period gratings written in a pure-silica photonic crystal fiber by the glass structure change," *J. Lightw. Technol.*, vol. 22, no. 2, pp. 625–630, Feb. 2004.

[19] V. I. Karpov, M. V. Grekov, E. M. Dianov, K. M. Golant, S. A. Vasiliev, O. I. Medvedkov, and R. R. Khrapko, "Mode-field converters and long-period gratings fabricated by thermo-diffusion in nitrogen-doped silica-core fibers," in *Proc. Optical Fiber Communication (OFC)*, San Diego, CA, 1998, pp. 279–280.

[20] P. Palai, M. N. Satyanarayan, M. Das, K. Thyagarajan, and B. P. Pal, "Characterization and simulation of long period gratings fabricated using electric discharge," *Opt. Commun.*, vol. 193, no. 1–6, pp. 181–185, 2001.

[21] T. Enomoto, M. Shigehara, S. Ishikawa, T. Danzuka, and H. Kanamori, "Long-period fiber grating in a pure-silica-core fiber written by residual stress relaxation," in *Proc. Optical Fiber Communication (OFC)*, San Diego, CA, 1998, pp. 277–278.

[22] M. Verhaegen, P. Orsini, D. Perron, X. Daxhelet, and S. Lacroix, "Long period gratings fabrication techniques," in *Proc. SPIE*, QC, Canada, 2000, vol. 4087, pp. 156–161.

[23] A. Malki, G. Humbert, Y. Ouerdane, A. Boukhenter, and A. Boudrioua, "Investigation of the writing mechansim of electric-arc-induced long-period fiber gratings," *Appl. Opt.*, vol. 42, no. 19, pp. 3776–3779, 2003.

[24] M. Kim, D. Lee, B. I. Hong, and H. Chung, "Performance characteristics of long-period fiber-gratings made from periodic tapers induced by electric-arc discharge," *J. Korean Phys. Soc.*, vol. 40, no. 2, pp. 369–373, 2002.

[25] E. M. Dianov, K. M. Golant, R. R. Khrapko, A. S. Kurkov, and A. L. Tomashuk, "Low-hydrogen silicon oxynitride optical fibers prepared by SPCVD," *J. Lightw. Technol.*, vol. 13, no. 7, pp. 1471–1474, Jul. 1995.

[26] P. K. Bachmann, W. Hermann, H. Wehr, and D. U. Wiechert, "Stress in optical waveguides. II. Fibers," *Appl. Opt.*, vol. 26, no. 7, pp. 1175–1182, 1987.

[27] W. Hermann, M. Hutjens, and D. U. Wiechert, "Stress in optical waveguides. 3. Stress induced index change," *Appl. Opt.*, vol. 28, no. 11, pp. 1980–1983, 1989.

[28] G. Rego, L. M. M. B. F. Santos, B. Schröder, P. V. S. Marques, J. L. Santos, and H. M. Salgado, "In situ temperature measurement of an optical fiber submitted to electric arc discharges," *IEEE Photon. Technol. Lett.*, vol. 16, no. 9, pp. 2111–2113, Sep. 2004.

[29] Y. Park, T. J. Ahn, Y. H. Kim, W. T. Han, U. C. Paek, and D. Y. Kim, "Measurement method for profiling the residual stress and the strain-optic coefficient of an optical fiber," *Appl. Opt.*, vol. 41, no. 1, pp. 21–26, 2002.

[30] Y. Park, U. C. Paek, and D. Y. Kim, "Complete determination of the stress tensor of a polarization-maintaining fiber by photoelastic tomography," *Opt. Lett.*, vol. 27, no. 14, pp. 1217–1219, 2002.

[31] B. L. Bachim and T. K. Gaylord, "Polarization-dependent loss and birefringence in long-period fiber gratings," *Appl. Opt.*, vol. 42, no. 34, pp. 6816–6823, 2003.

[32] I. K. Hwang, S. H. Yun, and B. Y. Kim, "Long-period fiber gratings based on periodic microbends," *Opt. Lett.*, vol. 24, no. 18, pp. 1263–1265, 1999.

[33] W. D. Kingery, H. K. Bowen, and D. R. Uhlmann, "Introduction to ceramics," in *Wiley Series on the Science and Technology of Materials*, vol. II. New York: Wiley, 1976, pp. 816–846.

[34] R. H. Doremus, "Viscosity of silica," *J. Appl. Phys.*, vol. 92, no. 12, pp. 7619–7629, 2002.

[35] Y. Mohanna, J. M. Saugrain, J. C. Rousseau, and P. Ledoux, "Relaxation of internal stresses in optical fibers," *J. Lightw. Technol.*, vol. 8, no. 12, pp. 1799–1802, Dec. 1990.

[36] P. L. Chu and T. Whitbread, "Stress transformation due to fusion splicing in optical fibre," *Electron. Lett.*, vol. 20, no. 14, pp. 599–600, Jul. 1984.

[37] B. I. Yakobson, P. J. Moyer, and M. A. Paesler, "Kinetic limits for sensing tip morphology in near-field scanning optical microscopes," *J. Appl. Phys.*, vol. 73, no. 11, pp. 7984–7986, 1993.

[38] V. I. Karpov, M. V. Grekov, E. M. Dianov, K. M. Golant, and R. R. Khrapko, "Ultra-thermostable long-period gratings written in nitrogen-doped silica fibers," in *Proc. Reliability Photonics Materials and Structures Symp.*, San Francisco, CA, 1998, pp. 391–396.

F. Dürr, photograph and biography not available at the time of publication.

G. Rego, photograph and biography not available at the time of publication.

P. V. S. Marques, photograph and biography not available at the time of publication.

Sergey L. Semjonov received the Ph.D. degree in physics from General Physics Institute, Russian Academy of Sciences, Moscow, Russia.

He is currently a Deputy Director of the Fiber Optics Research Center, General Physics Institute. His research interests cover different aspects of modern fiber optics: fabrication of preforms for optical fibers, the fiber drawing process, properties of polymer and hermetic coatings for optical fibers, strength and fatigue of optical fibers, influence of drawing conditions on optical properties of optical fibers, development of highly Ge- and P-doped fibers for Raman amplifiers and lasers, development of active fibers, photosensitivity of optical fibers, and microstructured fibers.

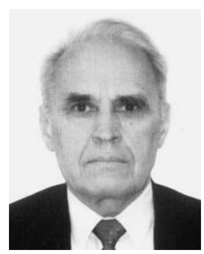

Evgeny M. Dianov (M'97) received the degree from Moscow State University, Moscow, Russia, in 1960.

He is director of the Fiber Optics Research Center of the Russian Academy of Sciences. He began his scientific career at the P.N. Lebedev Physical Institute, USSR Academy of Sciences. His research interests are in fiber optics, laser physics, and nonlinear optics.

Dr. Dianov is a member of MRS, a Fellow of OSA, and a full member of the Russian Academy of Sciences.

H. G. Limberger, photograph and biography not available at the time of publication.

R. P. Salathé (M'85–SM'88), photograph and biography not available at the time of publication.